Mass and charge attributes of heavy ion potentials obtained by inversion

C. Steward, K. Amos, and H. Leeb*
School of Physics, University of Melbourne, Parkville, Victoria 3052, Australia

L. J. Allen
School of Science & Mathematics Education, University of Melbourne, Parkville, Victoria 3052, Australia

H. Fiedeldey and S. A. Sofianos
Department of Physics, University of South Africa, P.O. Box 392, Pretoria, 0001 South Africa
(Received 30 April 1991)

Potentials are obtained using a WKB inverse scattering technique that is based upon S functions derived from strong absorption model fits to the elastic-scattering cross sections for 1503 MeV ^{16}O ions on ^{12}C, ^{40}Ca, ^{90}Zr, and ^{208}Pb. A systematic study of the mass (charge) dependence of the heavy ion nuclear potential at this energy is the result. In this context the dependence of the extracted nuclear potential on the assumed Coulomb interaction between the heavy ions is also considered. With increasing target mass the choice of representative Coulomb field is important in specification of the hadronic interaction component of the inversion potential.

I. INTRODUCTION

In a recent paper [1], we studied the radial forms of (local) nucleus-nucleus interactions as obtained by solution of the inverse scattering problem [2] at fixed energy. The elastic-scattering data from ^{12}C-^{12}C collisions at 360, 1016, 1449, and 2400 MeV were considered in particular and from which the basic input to the inversion method, the S functions, were determined using the strong absorption model of scattering as parametrized by McIntyre, Wang, and Becker [3]. Such a smooth parametrization of experimental data was particularly suitable for a systematic study of the energy dependence of the ^{12}C-^{12}C potentials, when used in conjunction with a semiclassical (WKB) inversion scheme [4]. That scheme permitted identification of the "sensitive" radial region wherein the potential was uniquely determined by the data and was valid for distances well inside the strong absorption radii. The resultant potentials were then used as input in a standard calculation [5] to solve the direct potential scattering problem and so recalculate phase shifts and S functions. The close agreement between those direct solution results (using the inverted potentials) and the original McIntyre parametrizations at all energies (360 to 2400 MeV) is a direct reflection of the propriety of the WKB inversion procedure as well as of the numerical methods used in its implementation. Consequently, we were able to conclude that the "sensitive" region centered around smaller radii with increasing energy and that, at a fixed radius (5 fm), the absorptive potential strength decreased with energy in contrast to some microscopic model predictions [6]. Also, the process produced potentials which had a short ranged repulsive component.

Herein we make a systematic study of mass variation effects in heavy ion scattering using inverted potentials. For that purpose the data [7] from the scattering of 1503 MeV ^{16}O ions from targets of ^{12}C, ^{40}Ca, ^{90}Zr, and ^{208}Pb were chosen for analysis. Those data are particularly suitable as previous analyses [8] have established that they can be well represented by McIntyre parametrizations of the scattering functions. Furthermore, the differential cross sections vary smoothly with target mass from a shape typical of Fraunhofer diffraction (^{12}C) to that of a characteristic "rainbow" scattering (^{208}Pb). Also for the ^{16}O-^{12}C case, an inversion using the eikonal approximation has been carried out in Ref. [9] and optical model studies have been done by Kobos, Brandan, and Satchler [10].

We also consider herein the role of the Coulomb potential as it is an important factor in any description of two heavy ions involved in a (nuclear) collision. Frequently a point charge approximation is used wherein the Coulomb interaction is approximated to that of a point projectile off of an effective, cutoff, uniform charge distribution. But the associated Coulomb potential is quite different to that between two finite, sharp cutoff distributions for radii less than the contact distance. Indeed, for ^{16}O on ^{208}Pb, double-folded sharp cutoff or Fermi distributions have been shown [11] to give Coulomb potentials that are more repulsive than the point charge approximation interaction within the touching radius by a factor that monotonically increases to 1.47 at zero separation radius. That study [11] showed but small variation between the double sharp cutoff and double-Fermi-folded potentials, however. The differences in nuclear interactions derived by inversion of scattering data according to which form of Coulomb field is extracted is considered herein.

In the next section the inversion method used to obtain interaction potentials is outlined and the results of our calculations are presented and discussed in Sec. III.

II. THE INVERSION METHOD FOR HEAVY ION POTENTIALS

Details of inverse scattering theory in the case of fixed energy and of the WKB approximation scheme that facilitates evaluation of inversion potentials have been given in the literature [2,4] and so only salient information will be given herein.

The inversion process begins with S-function values (or, equivalently, phase shifts) extracted from an analysis of differential cross-section data. A functional form must then be specified to encompass an angular momentum continuum. Therewith lies the value of the strong absorption models which allow for smooth parametrizations of scattering function or phase shifts as functions of $\lambda(=l+\frac{1}{2})$.

With $\delta(\lambda)$ being that phase-shift function, the classical deflection function is defined by

$$\theta(\lambda)=2\frac{d}{d\lambda}[\delta(\lambda)] , \tag{1}$$

in terms of which the WKB approach specifies a quasipotential

$$\begin{aligned} Q(\sigma)&=\frac{2E}{\pi}\int_{\sigma}^{\infty}[\theta(\lambda)/(\lambda^2-\sigma^2)^{1/2}]d\lambda \\ &\equiv\frac{4E}{\pi}\frac{1}{\sigma}\frac{d}{d\sigma}\left[\int_{\sigma}^{\infty}[\lambda\delta(\lambda)/(\lambda^2-\sigma^2)^{1/2}]d\lambda\right] \end{aligned} \tag{2}$$

with E and k being the center-of-mass energy and the wave number, respectively. The inverted potential is specified by the WKB approximation to be

$$V(r)=E\{1-\exp[-Q(\sigma)/E]\} \tag{3}$$

when conditions permit a one-to-one correspondence between r and σ via

$$r=(\sigma/k)\exp[Q(\sigma)/2E] . \tag{4}$$

To facilitate evaluations, it is convenient to make a rational ansatz [4,12] for the S matrix,

$$\delta(\lambda)=\frac{1}{2i}\ln[S(\lambda)]=\frac{1}{2i}\ln\left[\prod_{n=1}^{N}\frac{\lambda^2-\beta_n^2}{\lambda^2-\alpha_n^2}\right] \tag{5}$$

as the integrals in Eq. (2) can then be solved analytically. One needs simply then to map the S function to be inverted with a rational function representation. [In all of our calculations, eight pairs of poles (α_n,β_n) suffice to represent the S functions.] That S function is derived from the experimental one which is usually cast in the form

$$S_{\text{expt}}=S_{\text{nucl}}S_{\text{Coul}} \tag{6}$$

which involves point particle Coulomb S functions that are defined by

$$S_{\text{Coul}}(\lambda)=\Gamma(\lambda+\tfrac{1}{2}+i\eta)/\Gamma(\lambda+\tfrac{1}{2}-i\eta) \tag{7}$$

for a Sommerfeld parameter η. The asymptotic (Coulomb) behavior of S_{expt} is difficult to represent in a rational function form, whence a modified S function

$$S_{\text{sub}}=S_{\text{expt}}/S_{\text{back}} \tag{8}$$

is used instead. This is a background subtraction scheme [4] with S_{back} being an S function that in turn can be inverted. In our study of ^{12}C-^{12}C scattering [1], that background scattering function had the form $\exp[2i\delta(\lambda)]$ with a phase-shift function

$$2\delta_{\text{back}}(\lambda)=\eta\ln(\lambda^2+\lambda_c^2) , \tag{9}$$

where λ_c is a cutoff parameter. Inversion of S_{back} gives a potential, $V_{\text{back}}(r)$, which is a quasi-Coulomb potential since it behaves as r^{-1} for large radii. The use of a quasi-Coulomb background S functions is a significant aspect of the procedure as thereby the problems experienced by Kujawski [13] are alleviated. The choice of S_{back} [Eq. (9)] also ensures that V_{back} is not singular at the origin. We have used this prescription in our calculations with the values of 2.34, 7.8, 15.6, and 31.98 for λ_c for the scattering off of ^{12}C, ^{40}Ca, ^{90}Zr, and ^{208}Pb, respectively.

But with increasing target mass the Sommerfeld parameter increases and then a better representation of S_{back} may need to be used. One such phase-shift function is

$$\begin{aligned} 2\delta_{\text{back}}(\lambda)=&\eta\ln(\lambda^2+\lambda_c^2) \\ &-\eta(\lambda^2+\lambda_1^2)^{-1}(\lambda_c^2-\eta^2/6-1/12) \\ &+\eta^3/[6(\lambda^2+\lambda_1^2)^{3/2}] \end{aligned} \tag{10}$$

for which the WKB quasipotential is given by

$$\begin{aligned} \frac{1}{2E}Q_{\text{back}}(\sigma)=&\eta/(\sigma^2+\lambda_c^2)^{1/2}+\{\eta/2[(\sigma^2+\lambda_1^2)^{3/2}]\} \\ &\times(\lambda_c^2-\eta^2/6-1/12) \\ &-(\eta^2/3\pi)/[(\sigma^2+\lambda_1^2)^2] . \end{aligned} \tag{11}$$

Such extensions were not necessary in our calculations however.

One must then specify the empirical S function, and a procedure that worked well in our previous studies [1] is to use a physically motivated prescription for the "nuclear" part of the experimental S function [Eq. (6)]. Of a number of forms, that of McIntyre, Wang, and Becker [3] is particularly useful. With such S functions, the method can be used to obtain $Q_{\text{sub}}(\sigma)$ with which the complete quasipotential is

$$Q(\sigma)=Q_{\text{sub}}(\sigma)+Q_{\text{back}}(\sigma) \tag{12}$$

and the inverted potential at radii defined by Eq. (4) follows. This inverted potential, $V_{\text{inv}}(r)$, we resolve as

$$V_{\text{inv}}(r)=V_{\text{nuc}}(r)-V_{\text{Coul}}^{FS}(r) , \tag{13}$$

where the superscript $[FS]$ indicates that this Coulomb potential should be that between two extended (finite size) charged objects [11]. This choice is to be contrasted with that of a point particle interacting with an extended charge sphere, the point charge approximation, for which

$$V_{\text{Coul}}^{\text{pca}}(r)=\begin{cases}2\eta/r & \text{for } r>R_{pt}\ , \\ \dfrac{\eta}{R_{pt}}\left[3-\dfrac{r^2}{R_{pt}^2}\right] & \text{for } r<R_{pt}\ .\end{cases} \tag{14}$$

For heavy ion collisions, standard optical model analyses frequently use

$$R_{pt}=r_c(A_P^{1/3}+A_T^{1/3}) \tag{15}$$

with r_c in the range 1.1 to 1.3 fm.

III. RESULTS OF CALCULATIONS

The nuclear components of heavy ion interactions that are important in direct scattering calculations are those that lie within a sensitive radial region. That region varies with both particle masses and incident energy but invariably lies around characteristic radii such as the strong absorption radii. For 1503 MeV ^{16}O ions upon various targets a set of characteristic radii are given in Table I. Therein the strong absorption radii (R_{SA}) and contact radii (R_C) are as specified by Roussel-Chomaz *et al* [7]. Also given are the radii at which inverted potentials have their deepest well values and the sensitive radial regions as defined by notch testing of standard optical model analyses of the relevant differential cross-section data. Clearly, the sensitive radial regions extend well inside of the strong absorption radii but, it is to be stressed, not very far within the contact radii.

In Fig. 1, the original (McIntyre parametrized) S functions are compared with those recalculated using the inversion potentials in the Schrödinger equation. The original functions are depicted by the continuous lines with the real and imaginary parts of those functions presented on the top and bottom sections of the figure, respectively. The "reconstituted" results, calculated using inversion potentials [the background S functions defined in Eq. (10) were used in the inversion procedure] in the Schrödinger equation, are indistinguishable from them on these scales. The (original) S functions were specified by Mermaz in his analyses of data [8] and the relevant parameter values are listed for completeness in Table II. The center-of-mass energies and wave numbers are listed in the first two rows and the Sommerfeld parameter values are given in the third row. The grazing angular momentum (l_g) and diffusivity (Δ_g) that define the modulus of the McIntyre S function then follow. The scaling weight (μ), grazing angular momentum ($l_{g'}$), and diffusivity ($\Delta_{g'}$), that complete the five parameter McIntyre forms, are listed in the last three rows.

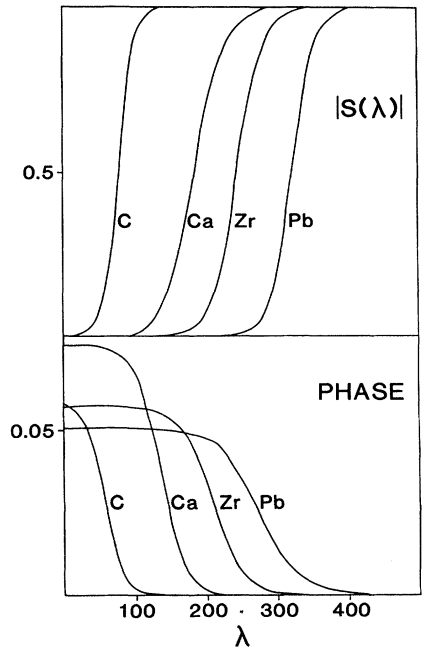

FIG. 1. The S functions for the scattering of 1503 MeV ^{16}O ions from ^{12}C, ^{40}Ca, ^{90}Zr, and ^{208}Pb. The continuous curves are the forms obtained by fitting differential cross sections with a McIntyre parametrized, strong absorption model of scattering. They also correspond at this magnification to those obtained from solutions of Schrödinger equations with the inversion potentials.

The nuclear potentials obtained from the inversion scheme are displayed in Fig. 2. Therein the real and imaginary components of those potentials are given in the top and bottom sections, respectively, with each target

TABLE I. Characteristic radii for 1503 MeV ^{16}O ions scattering from various nuclei. Units are Fermi.

	^{12}C	^{40}Ca	^{90}Zr	^{208}Pb
R_S (strong absorption) [a] $[\approx 1.3\,(A_1^{1/3}+A_2^{1/3})]$	6.2	7.9	9.3	10.9
R_C (contact) $[=1.1\,(A_1^{1/3}+A_2^{1/3})]$	5.3	6.5	7.7	9.2
R_D (deepest real potential)	2.8	4.8	6.6	8.4
R_I (sensitive radii) [a]	3 to 6	6 to 8.6	6.9 to 10.5	9 to 11.5

[a]Values taken from Ref. [7].

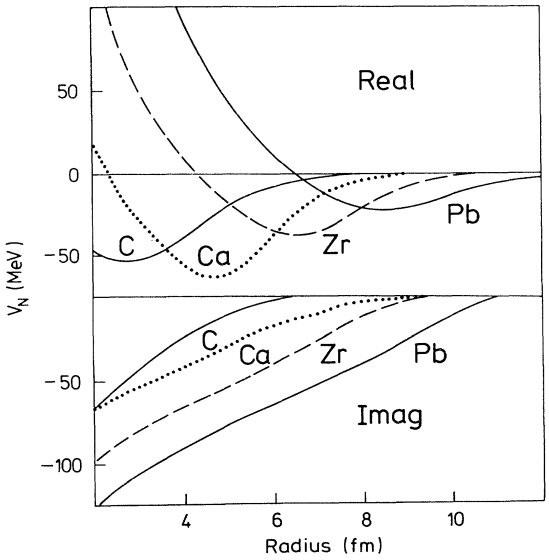

FIG. 2. The potentials obtained using the WKB inversion method. The real and imaginary components are shown in the top and bottom sections, respectively, and the results for each target are identified by their nuclear symbols.

identified. These potentials were obtained using the Coulomb potential from [Eq. (14)] to facilitate comparison with conventional optical model (phenomenological) potentials. The potentials are given from 2 fm; a limit that ensures all potentials are displayed far inside of their "sensitive" radial regions. Characteristically, all the real parts of these potentials are attractive wells modulated by a short-range repulsion. Such was also found in our previous study [1]. The depths of the attractive wells vary with mass with ^{40}Ca being the deepest and thereafter showing a monotonic decrease for heavier targets. But the well bottoms are far inside both the strong absorption radii and the contact radii. Those characteristic radii and the sensitive radial regions for elastic scattering of 1503 MeV ^{16}O ions off of the four targets are given in Table I. Clearly, the noticeable onset of the repulsion in each of these inverted potentials is well inside the sensitive radial region for scattering. At those distances, also, the absorption is very strong. Consequently, the short-ranged details of the inverted potentials by themselves contribute little to calculations of differential cross sections. We established that fact by setting all positive values of those interaction potentials arbitrarily to zero and used the resulting, modified, potentials to calculate cross sections. They were not sensibly different from the results obtained using the unmodified interactions. Thereby we confirmed the lower limits of the sensitive radial regions as specified by current data.

The imaginary components of the inversion potentials vary with target mass as well. This is evident from Table III wherein the strengths of the imaginary potentials at both the contact and strong absorption radii are given. The ratios of real to imaginary potentials at these radii are also listed. The ^{40}Ca results are unusual defying the trends set by the others. Those trends are that the rate increase in absorption strengths between R_s and R_c changes markedly with target mass and that the real potential becomes relatively more important than the imaginary potential with increasing radius and with increasing mass. Clearly through the sensitive radial regions absorption processes are more important for ^{208}Pb than for ^{12}C but that variation between those masses is not a simple function. The general mass variation of these potentials are evident from the shapes of the differential cross sections changing from one reminiscent of Fraunhofer diffraction to a characteristic rainbow form.

Taken in conjunction with the energy variation of inversion potentials reported previously [1], these mass variation results indicate that simple functional forms, e.g., a Woods-Saxon function with smooth E and A dependent parameters, are unlikely to be appropriate heavy ion interactions. It also suggests that attempts to define heavy ion interactions using microscopic models of nuclear structure must also take into account appropriate nuclear dynamics with pertinent energy dependent off-shell two nucleon G matrices and allowance for Pauli blocking [14] at least. Our ^{16}O-^{12}C potential agrees well

TABLE II. McIntyre S matrix parameter values for 1503 MeV ^{16}O ions.

	Mermaz				Fit
	C	Ca	Zr	Pb	Pb
$E_{c.m.}$	644	1073	1276	1396	1396
$k_{c.m.}$	14.6	24.3	28.9	31.2	31.2
η	0.78	2.6	5.2	10.7	10.7
l_g	75.8	183.0	244.1	319.7	321.1
Δ_g	10.3	20.3	17.1	15.2	20.0
μ	3.4	4.4	3.3	2.9	1.1
$l_{g'}$	56.1	133.9	206.4	271.2	306.0
$\Delta_{g'}$	13.4	17.5	21.8	30.2	14.8

TABLE III. The imaginary potential strengths (W) and the ratio of real to imaginary potentials at the contact and strong absorption radii.

		W (MeV)	(V/W)
^{12}C	R_c	−9.37	1.82
	R_s	−3.46	2.06
^{40}Ca	R_c	−15.85	1.72
	R_s	−6.45	0.81
^{90}Zr	R_c	−18.95	1.54
	R_s	−3.84	1.52
^{208}Pb	R_c	−26.67	0.88
	R_s	−4.52	1.47

with that obtained in the eikonal approximation in Ref. [9].

As has been noted, the Coulomb interaction between heavy ions usually is represented by a point charge projectile interacting with a charged sphere of radius the sum of the two ion radii. The associated potential for the ^{16}O-^{12}C system is displayed by the dash line in Fig. 3. A better representation is to use two uniformly charged spheres, for which the Coulomb potential is as shown by the continuous line. (It has been shown recently [15] that the Coulomb interaction between two uniformly charged heavy ions has a simpler form than given by deVries and Clover [11].) Clearly, the two differ, notably inside of the strong absorption radius, and with the two sphere interaction being more repulsive as has been shown previously [11]. While the variation between these potentials occurs only within the Coulomb radius (5.8 fm), which for 1503 MeV ^{16}O ions on ^{12}C is essentially the strong absorption radius as well, that variation does noticeably affect what one extracts as the nuclear potential from the inversions. The difference is shown in Fig. 4 wherein the real parts of the nuclear potentials extracted using the point charge and finite charge models' Coulomb potentials are shown by the dash and continuous curves, respectively. The more realistic charge distribution case gives a nuclear interaction noticeably more attractive at small separation radii and with differences that are still important in the sensitive radial region. Those sensitive radial regions [7] are displayed in Fig. 4 by the horizontal arrows. The strong absorption radii are designated by R_s. Clearly the largest differences occur in regions of little significance in so far as influence upon the analyses of current measured data are concerned. But there are nontrivial differences between the two specifications of the nuclear potentials within the sensitive radial regions. Differences of 10–15 % can occur therein. Thus the choice of Coulomb interaction form is important if one wishes to compare estimates of heavy ion nuclear interactions obtained from microscopic model calculations based upon two nucleon G matrices.

The input to our WKB inversion scheme are S functions. We chose those of McIntyre form and with parameter values specified previously by Mermaz [8]. But, for the scattering of 1503 MeV ^{16}O ions from ^{208}Pb, use of that inverted potential in a nonrelativistic Schrödinger equation did not give a very good fit to the ratio to Rutherford cross-section data. The result is shown by the dashed curve in Fig. 5. We therefore made a new parameter search to optimize the fit to that data. The

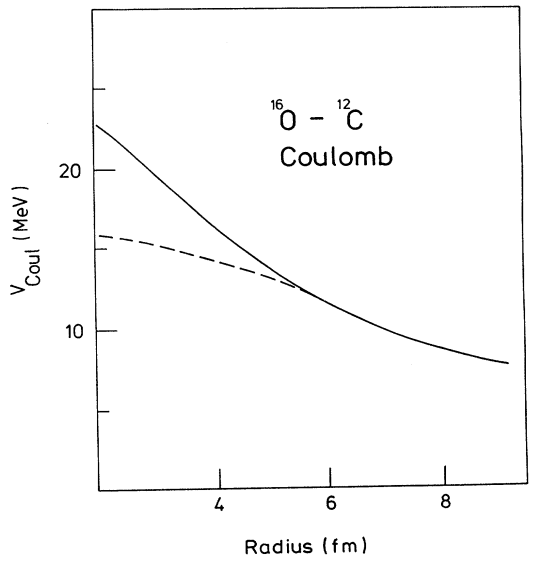

FIG. 3. The ^{16}O-^{12}C Coulomb potentials. The Coulomb potentials for a point charge projectile approximation [Eq. (14)] and for two uniformly charged spheres [11] in collision are displayed in this figure and by the dash and continuous lines, respectively.

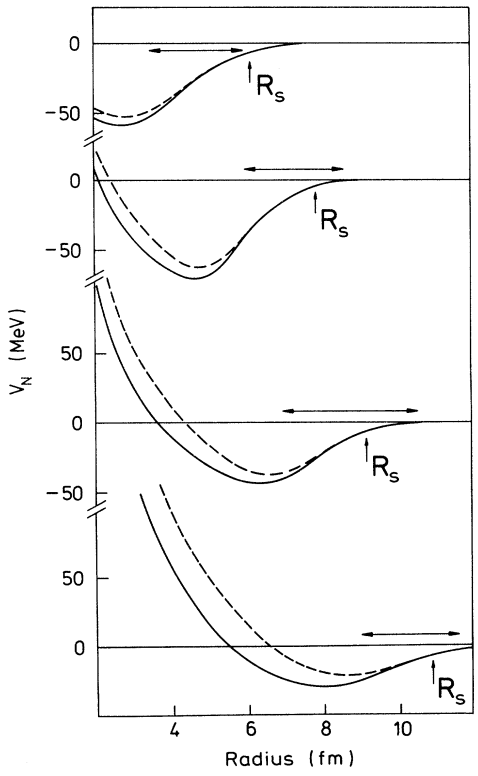

FIG. 4. The real parts of the nuclear potentials obtained by inversion of the 1503 MeV ^{16}O scattering S functions with point particle approximation Coulomb [Eq. (14)] (dash) and finite charge Coulomb potential [11] subtractions and for each of the targets as indicated. The strong absorption radii are defined by the vertical arrows while the sensitive radial regions are indicated by the horizontal arrow range.

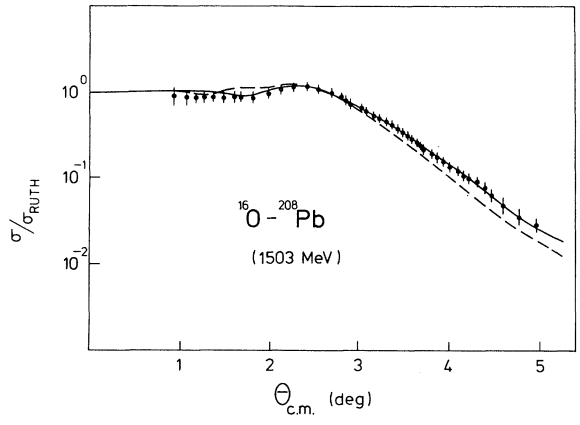

FIG. 5. The differential cross sections (ratio to Rutherford) from 1503 MeV ^{16}O ions elastically scattered from ^{208}Pb. The dash curve gives the result obtained using the Mermaz parameter values, to specify the S function in a (nonrelativistic) calculation. The solid curve is the result of our search to optimize the McIntyre S function parametrization.

McIntyre parameter values listed in the last column of Table II are the result. With that new S function, inversion gave a potential whose use in a Schrödinger equation led to the cross section displayed by the continuous line in Fig. 5. It is an excellent fit to the measured data. The potentials themselves are shown in Fig. 6. The real and imaginary parts of the "Mermaz" (dash curves) and "fitted" (continuous lines) potentials are shown therein in the top and bottom sections, respectively. The fitted potential is significantly weaker than the "Mermaz" one and through the sensitive radius region in particular. The fitted potential has more significant repulsion effects in the real part with some shape variation from that obtained starting with the Mermaz S function. That latter shape variation, however, is not in the current sensitive radius region. More data of quality at larger scattering angles are needed to probe the nuclear interaction at such distances.

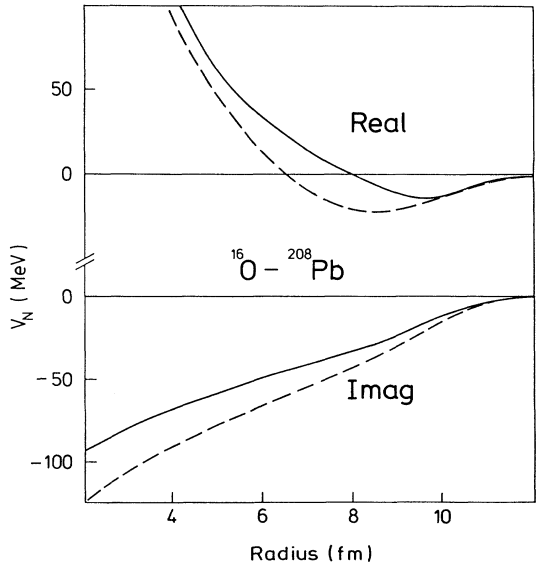

FIG. 6. A comparison of the ^{16}O-^{208}Pb inverted potentials obtained using Mermaz's and our optimized set of parameter values in a McIntyre form for the input S functions.

IV. CONCLUSIONS

The mass dependence of the interaction of ^{16}O ions scattering off ^{12}C, ^{40}Ca, ^{90}Zr, and ^{208}Pb has been studied systematically using a WKB inversion method at fixed energy and starting from a strong absorption model for the scattering function. With increasing mass of the target, absorption onsets at increasing radii. Also the strengths of the absorptive parts of the potentials relative to the real parts increase with mass so that, for the heaviest target, ^{208}Pb, absorption dominates. The strong absorption model (SAM) also implies an increasing short-range repulsive, component in the real potentials, with onset at larger radii as the mass increases. But the major variation with target mass is the relative importance of the refractive (real) and absorptive (imaginary) potentials. For the light targets, at this energy, refraction is particularly effective and the consequence is a Fraunhoffer diffractive pattern to differential cross sections. With increasing mass of the target (above Ca in our examples) absorption and Coulomb repulsion become relatively more important to the effect that the associated differential cross sections have a shape characteristic of Fresnel diffraction.

It was shown that the usual assumption for the Coulomb field (of a point charge scattering off an effective finite size charge distribution) results in a nuclear potential, extracted by inversion, which is substantially different from that obtained if we assume that both projectile and target have finite sized charge distributions. This is particularly so for the heavy, large Z targets. But, irrespective of the type of Coulomb interaction assumed, the real part of the nuclear potentials obtained by inversion all are mixtures of a long-range attraction and a short-ranged repulsion. Based upon current data, however, the exact details of that repulsion at small radii (inside the current sensitive radius regions) are not of significance. But the variations with target mass, as well as with energy as we found previously, of the inversion potentials through the sensitive radial regions seem not to be of a simple form. We do not believe that a Woods-Saxon function with parameter values that vary smoothly with mass and energy can be a sufficiently realistic representation of heavy ion interactions.

Finally, we note that the method of specifying the input S function is important. As our inversion scheme is based upon the (nonrelativistic) Schrödinger equation, the

process of defining the S functions from fits to measured data should be consistent. In the case of ^{16}O-^{208}Pb scattering the McIntyre parameter values taken from the literature were not optimal whence the potential obtained from inversion of that S function differed noticeably from that found with input S functions that we tuned to best fit the data.

ACKNOWLEDGMENTS

One of us (H.L.) gratefully acknowledges the support and hospitality that he received during a period of research field work at the University of Melbourne. Another (L.J.A.) acknowledges the support and hospitality of colleagues during a stay at the University of South Africa.

*On leave from Institute für Kernphysik, Technische Universität Wien, A-1040 Wien, Austria.

[1] L. J. Allen, K. Amos, C. Steward, and H. Fiedeldey, Phys. Rev. C **41**, 2021 (1990).

[2] K. Chadan and P. C. Sabatier, *Inverse Problems in Quantum Scattering Theory*, Second Edition (Springer, Berlin, 1988), and references cited therein.

[3] J. A. McIntyre, K. H. Wang, and L. C. Becker, Phys. Rev. **117**, 1337 (1960).

[4] H. Fiedeldey, R. Lipperheide, K. Naidoo, and S. A. Sofianos, Phys. Rev. C **30**, 434 (1984).

[5] J. Raynal, Phys. Rev. C **23**, 2571 (1981) and Program ECIS88, C.E.A., Saclay report, 1982 (unpublished).

[6] N. Ohtsuka, M. Shabshiry, R. Linden, H. Müther, and A. Faessler, Nucl. Phys. **A490**, 715 (1988).

[7] P. Roussel-Chomaz, N. Alamanos, F. Auger, J. Barrette, B. Berthier, B. Fernandez, L. Papineau, H. Doubre, and W. Mittig, Nucl. Phys. **A477**, 345 (1988).

[8] M. C. Mermaz, Z. Phys. A **321**, 613 (1985).

[9] R. da Silveira and Ch. Leclercq-Willain, Orsay Report IPNO/TH 86-38 (unpublished).

[10] A. M. Kobos, M. E. Brandan, and G. R. Satchler, Nucl. Phys. **A487**, 457 (1988).

[11] R. M. De Vries and M. R. Clover, Nucl. Phys. **A243**, 528 (1975).

[12] K. Naidoo, H. Fiedeldey, S. A. Sofianos, and R. L. Lipperheide, Nucl. Phys. **A419**, 13 (1984).

[13] E. J. Kujawski, Phys. Rev. C **6**, 709 (1972); **8**, 100 (1973).

[14] Dao Tien Khoa, A. Faessler, and N. Ohtsuka, J. Phys. G **16**, 1253 (1990); M. E. Brandan and G. R. Satchler, Nucl. Phys. **A487**, 477 (1988).

[15] M. W. Kermode, M. M. Mustafa, and N. Rowley, J. Phys. G **16**, L299 (1990).